POLISH MARITIME RESEARCH 2(86) 2015 Vol. 22; pp. 71-78
10.1515/pomr-2015-0019

SIMPLIFIED PROCEDURE FOR THE FREE VIBRATION ANALYSIS OF RECTANGULAR PLATE STRUCTURES WITH HOLES AND STIFFENERS

Dae Seung Cho, Ph.D.
Pusan National University, Busan, Korea

Nikola Vladimir, Ph.D.
University of Zagreb, Zagreb, Croatia

Tae Muk Choi, Ph.D.
Createch Co. Ltd., Busan, Korea

ABSTRACT

Thin and thick plates, plates with holes, stiffened panels and stiffened panels with holes are primary structural members in almost all fields of engineering: civil, mechanical, aerospace, naval, ocean etc. In this paper, a simple and efficient procedure for the free vibration analysis of such elements is presented. It is based on the assumed mode method and can handle different plate thickness, various shapes and sizes of holes, different framing sizes and types as well as different combinations of boundary conditions. Natural frequencies and modes are determined by solving an eigenvalue problem of a multi-degree-of-freedom system matrix equation derived by using Lagrange's equations. Mindlin theory is applied for a plate and Timoshenko beam theory for stiffeners. The applicability of the method in the design procedure is illustrated with several numerical examples obtained by the in-house developed code VAPS. Very good agreement with standard commercial finite element software is achieved.

Keywords: energy approach, plate with hole, stiffened panel, thick plate, VAPS software, free vibration analysis

INTRODUCTION

Different kinds of rectangular plate systems, for instance thick plates, plates with holes, stiffened panels, stiffened panels with holes etc., can be found in all fields of engineering: civil, mechanical, aerospace, naval, ocean, etc. The free vibration analysis of such elements is an important issue in the design process. The finite element method (FEM) is nowadays an advanced and widespread numerical tool for that purpose and gives a complete solution to the vibration analysis of complex systems. However, the preparation of a model is a rather time-consuming task which makes it reasonable to apply it, usually, at the end of the detail design stage, after all the structural members, their dimensions and boundary conditions have been completely defined. In this sense, at the preliminary design stage when the principal dimensions are being selected, it is useful to have some simplified method at hand.

Although the thick plate theory represents an issue for very long time, i.e. since the first works published by Reissner and Mindlin [1 ÷ 2], its complexity caused by shear influence and rotary inertia makes it still a challenging problem, and it is not surprising that there are numerous references on this topic. As can be seen in the literature survey presented by Liew et al. [3], many concepts, based both on analytical and numerical solution of equilibrium equations, have been worked out. There are various analytical methods whose main drawback is the applicability limited only to simply supported plates or plates with two opposite edges simply supported. They differ depending on which functions are kept as fundamental when reducing the system of differential equations of motion. Some methods operate with three, two, or even one function [4 ÷ 5]. For the vibration analysis of plates with arbitrary edge constraints, including also elastically restrained edges, different variants of the Rayleigh-Ritz (energy) method are on disposal. The accuracy of such methods is dependent on the chosen set of orthogonal functions for the assumed natural modes, where two dimensional polynomials or static Timoshenko beam deflection functions, [6] and [7 ÷ 9], respectively, can be used. In the context of FEM application in the vibration analysis of thick plate, a shear locking problem should be mentioned. Namely, in the Mindlin thick plate theory shear deformations are taken into account, and the application of ordinary low-order finite element is not capable to reproduce pure bending modes in the limiting case of a thin plate. This shear locking problem arises due to

inadequate dependence between the transverse deflection and two rotations. However, it has been successfully overcome by different types of procedures developed in recent years [10 ÷ 15].

An overview of methods for the vibration analysis of plates with holes is presented in [16], where the advantages and drawbacks of different methods, for instance the finite difference method [17], the Rayleigh-Ritz [18] and the optimized Rayleigh-Ritz method [19], FEM [20], etc., are discussed.

In the case of stiffened panels, to the authors' knowledge, there are a rather limited number of references to their dynamic analysis [21]. Generally, the most common methods applied to the vibration analysis of stiffened plates can be classified into closed-bound solutions, energy methods, and other numerical methods [21 ÷ 22].

In the case of the vibration analysis of stiffened panels with holes, only a few references, based on the application of the finite element method, are available. Sivasubramonian et al. [23] studied the effect of curvature and hole size on square panels with different boundary conditions applied to the shell element having seven degrees of freedom per node. Sivasubramonian et al. [24] also applied the same finite element to both stiffened and unstiffened plate with holes and presented comparative results. Recently, Srivastava [25] applied the finite element method to the vibration analysis of stiffened panels with a single hole and different boundary conditions, under partial edge loading.

This paper reviews the application of the assumed mode method to the vibration analysis of thick plates, plates with multiple holes, and stiffened panels. In addition, expressions for partial stiffeners and carlings are presented. It should be emphasized that only the flexural global modes of the above structures are considered.

Further, it is shown that the method can also be applied to stiffened panels with holes. The effect of stiffeners is taken into account by adding their potential and kinetic energy to the potential and kinetic energy of the plate, respectively. Similarly to this, the potential and kinetic energies of the holes are subtracted from the corresponding energies of the plate, respectively. In this sense different combinations of topologies can be taken into account by appropriate manipulation with potential and kinetic energies of particular components. The computational tool VAPS (Vibration Analysis of Plate Systems) based on the assumed mode method has been developed and different numerical examples are analysed. The developed procedure is shown to be very simple, fast and accurate. Its main advantage in comparison with FEM is very fast model preparation. It is therefore recommended for practical use in the preliminary design phase of plate-like systems, when effects of different topologies, materials, boundary conditions, etc. on dynamic response are being investigated.

OUTLINE OF THE MATHEMATICAL FORMULATION

The mathematical model for the vibration analysis of different plate systems based on the assumed mode method is already applied in [8], [16] and [21], and here its outline with some extensions is given. The Mindlin thick plate theory [2] which takes shear influence and rotary inertia into account is adopted in the model. The Mindlin theory operates with three general displacements, i.e. plate deflection w, and angles of cross-section rotation about the x and y axes, ψ_x and ψ_y, respectively.

In the derivation of the eigenvalue problem which is necessary to obtain the free response, the Lagrange's equation is applied. In this sense the expression for total system potential, V, and kinetic energy, T, respectively is required. In the case of a solid plate, the total system energy is equal to the plate energy:

$$V = V_p, \quad T = T_p \tag{1}$$

Potential and kinetic energies for the plate with holes yield:

$$V = V_p - V_h, \quad T = T_p - T_h, \tag{2}$$

and for the stiffened panel

$$V = V_p + V_s, \quad T = T_p + T_s \tag{3}$$

Analogously to this, one can write for the potential and kinetic energy of a stiffened panel with holes:

$$V = V_p + V_s - V_h, \quad T = T_p + T_s - T_h \tag{4}$$

In the above expressions V_p is the plate strain energy, V_s represents the strain energy of stiffeners and V_h is the strain energy of a hole. Similarly, T_p is the plate kinetic energy, while T_s and T_h are the kinetic energies of the stiffeners and hole, respectively.

Energy of rectangular plate

By introducing the dimensionless parameters $\zeta = x/a$, $\eta = y/b$, $\alpha = a/b$ and $S = kGh/D$ for a rectangular plate of length a and width b with arbitrary boundary conditions, one can write for its potential and kinetic energies [8]:

$$\begin{aligned} V_p = \frac{D}{2\alpha}\int_0^1\int_0^1 \Bigg[& \left(\frac{\partial \psi_\xi}{\partial \xi}\right)^2 + \alpha^2\left(\frac{\partial \psi_\eta}{\partial \eta}\right)^2 \\ & + 2\nu\alpha\frac{\partial \psi_\xi}{\partial \xi}\frac{\partial \psi_\eta}{\partial \eta} + \frac{1-\nu}{2}\left(\alpha\frac{\partial \psi_\xi}{\partial \eta} + \frac{\partial \psi_\eta}{\partial \xi}\right)^2 \\ & + S\left(\left(\frac{\partial w}{\partial \xi} - a\psi_\xi\right)^2 + \alpha^2\left(\frac{\partial w}{\partial \eta} - b\psi_\eta\right)^2\right)\Bigg] \mathrm{d}\xi \mathrm{d}\eta \\ & + \int_0^1 \left[K_{Rx1}\psi_\xi^2(0,\eta) + SK_{Tx1}w^2(0,\eta)\right]\mathrm{d}\eta \\ & + \alpha^2\int_0^1 \left[K_{Ry1}\psi_\eta^2(\xi,0) + SK_{Ty1}w^2(\xi,0)\right]\mathrm{d}\xi \\ & + \int_0^1 \left[K_{Rx2}\psi_\xi^2(1,\eta) + SK_{Tx2}w^2(1,\eta)\right]\mathrm{d}\eta \\ & + \alpha^2\int_0^1 \left[K_{Ry2}\psi_\eta^2(\xi,1) + SK_{Ty2}w^2(\xi,1)\right]\mathrm{d}\xi, \end{aligned} \tag{5}$$

$$T_p = \frac{\rho ab}{2}\int_0^1\int_0^1\left[h\left(\frac{\partial w}{\partial t}\right)^2 + \frac{h^3}{12}\left(\frac{\partial \psi_\xi}{\partial t}\right)^2 + \frac{h^3}{12}\left(\frac{\partial \psi_\eta}{\partial t}\right)^2\right]\mathrm{d}\xi\mathrm{d}\eta \quad (6)$$

where $K_{Tx1} = (k_{Tx1}a/kGh)$, $K_{Tx2} = (k_{Tx2}a/kGh)$, $K_{Ty1} = (k_{Ty1}a/kGh)$ and $K_{Ty2} = (k_{Ty2}a/kGh)$ are dimensionless stiffness values at x = 0, x = a, y = 0 and y = b, respectively, and correspond to the translational spring constants per unit length k_{Tx1}, k_{Tx2}, k_{Ty1} and k_{Ty2} [8],[16]. In the same manner, $K_{Rx1} = (k_{Rx1}a/D)$, $K_{Rx2} = (k_{Rx2}a/D)$, $K_{Ry1} = (k_{Ry1}b/D)$ and $K_{Ry2} = (k_{Ry2}b/D)$ are for the rotational spring constants per unit length k_{Rx1}, k_{Rx2}, k_{Ry1} and k_{Ry2} at boundaries, respectively. The following quantities are related to the x direction: a, k_{Tx1}, k_{Tx2}, k_{Rx1} and k_{Rx2}. Other quantities (b, k_{Ty1}, k_{Ty2} k_{Ry1} and k_{Ry2}) are relevant for the y direction [16]. Also ρ represents plate material density, h is the plate thickness, k is the shear correction factor, while ν is the Poisson's ratio. Further, D represents plate flexural stiffness $D = Eh^3/(12(1-\nu^2))$, while E and G = E/(2(1+ν)) are Young's and shear moduli, respectively.

Energy of holes

In a similar way as for the plate without holes, one can write for the potential and kinetic energy of the rectangular hole shown in Fig. 1a, respectively:

$$V_{rh} = \frac{D}{2\alpha}\int_{y_{ro}-b_{ro}}^{y_{ro}+b_{ro}}\int_{x_{ro}-a_{ro}}^{x_{ro}+a_{ro}}\left[\left(\frac{\partial \psi_\xi}{\partial \xi}\right)^2 + \alpha^2\left(\frac{\partial \psi_\eta}{\partial \eta}\right)^2 + 2\nu\alpha\frac{\partial \psi_\xi}{\partial \xi}\frac{\partial \psi_\eta}{\partial \eta} + \frac{1-\nu}{2}\left(\alpha\frac{\partial \psi_\xi}{\partial \eta} + \frac{\partial \psi_\eta}{\partial \xi}\right)^2 + S\left(\left(\frac{\partial w}{\partial \xi} - a\psi_\xi\right)^2 + \alpha^2\left(\frac{\partial w}{\partial \eta} - b\psi_\eta\right)^2\right)\right]\mathrm{d}\xi\mathrm{d}\eta \quad (7)$$

$$T_{rh} = \frac{\rho ab}{2}\int_{y_{ro}-b_{ro}}^{y_{ro}+b_{ro}}\int_{x_{ro}-a_{ro}}^{x_{ro}+a_{ro}}\left[h\left(\frac{\partial w}{\partial t}\right)^2 + \frac{h^3}{12}\left(\frac{\partial \psi_\xi}{\partial t}\right)^2 + \frac{h^3}{12}\left(\frac{\partial \psi_\eta}{\partial t}\right)^2\right]\mathrm{d}\xi\mathrm{d}\eta \quad (8)$$

In Fig. 1a, xrh and yrh denote the longitudinal and transverse coordinates of the rectangular hole centre of gravity, and arh and brh are equal to one half of its length and width. Analogously to the rectangular hole, the potential and kinetic energies of the elliptical hole shown in Fig. 1b yield:

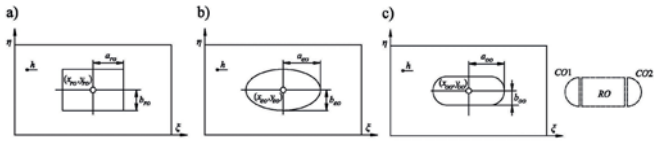

Fig. 1. Rectangular plates with different hole shapes; a) rectangular, b) elliptic, c) oval [16]

$$V_{eh} = \frac{D}{2\alpha}\int_{y_{eo}-b_{eo}}^{y_{eo}+b_{eo}}\int_{x_{eo}-a_{eo}\sqrt{1-\left(\frac{\eta-y_{eo}}{b_{eo}}\right)^2}}^{x_{eo}+a_{eo}\sqrt{1-\left(\frac{\eta-y_{eo}}{b_{eo}}\right)^2}}\left[\left(\frac{\partial \psi_\xi}{\partial \xi}\right)^2 + \alpha^2\left(\frac{\partial \psi_\eta}{\partial \eta}\right)^2 + 2\nu\alpha\frac{\partial \psi_\xi}{\partial \xi}\frac{\partial \psi_\eta}{\partial \eta} + \frac{1-\nu}{2}\left(\alpha\frac{\partial \psi_\xi}{\partial \eta} + \frac{\partial \psi_\eta}{\partial \xi}\right)^2 + S\left(\left(\frac{\partial w}{\partial \xi} - a\psi_\xi\right)^2 + \alpha^2\left(\frac{\partial w}{\partial \eta} - b\psi_\eta\right)^2\right)\right]\mathrm{d}\xi\mathrm{d}\eta \quad (9)$$

$$T_{eh} = \frac{\rho ab}{2}\int_{y_{ro}-b_{ro}}^{y_{ro}+b_{ro}}\int_{x_{eo}-a_{eo}\sqrt{1-\left(\frac{\eta-y_{eo}}{b_{eo}}\right)^2}}^{x_{eo}+a_{eo}\sqrt{1-\left(\frac{\eta-y_{eo}}{b_{eo}}\right)^2}}\left[h\left(\frac{\partial w}{\partial t}\right)^2 + \frac{h^3}{12}\left(\frac{\partial \psi_\xi}{\partial t}\right)^2 + \frac{h^3}{12}\left(\frac{\partial \psi_\eta}{\partial t}\right)^2\right]\mathrm{d}\xi\mathrm{d}\eta \quad (10)$$

If one introduces $x_{eh} = y_{eh}$ in the equations (9) and (10), the potential and kinetic energies of the circular hole are obtained. As in previous case, x_{eh} and y_{eh} in Fig. 1b denote the longitudinal and transverse coordinates of the elliptic hole centre of gravity, while a_{eh} and b_{eh} are the major and minor semi-axes of the hole, respectively. An oval hole, which can often be found in ships and offshore structures, can be treated as a combination of rectangular and semi-circular holes, Fig. 1c, where x_{oh} and y_{oh} are the longitudinal and transverse coordinates of the oval hole centre of gravity, while aoh and boh are equal to one half of its length and width, respectively.

In this way, its potential and kinetic energies can be written in the following form:

$$T_{oh} = T_{ch1} + T_{rh} + T_{ch2}, \qquad V_{oh} = V_{ch1} + V_{rh} + V_{ch2} \quad (11)$$

and can be calculated with the above-listed formulae. In addition, the procedure can be applied to multiple holes, but then the hole potential and kinetic energies have to be calculated separately, and subtracted from the corresponding energies of the plate without holes.

Energy of stiffeners

The potential and kinetic energy of stiffeners placed in the longitudinal and transverse directions yield:

$$V_s = \frac{a}{2}\sum_{r=1}^{n_x}\left[\int_0^1\left(\frac{EI_{x_r}}{a^2}\left(\frac{\partial \psi_\xi}{\partial \xi}\right)^2 + K_{x_r}A_{wx_r}G\left(\frac{\partial w}{a\partial \xi} - \psi_\xi\right)^2 + \frac{GJ_{x_r}}{a^2}\left(\frac{\partial \psi_\eta}{\partial \xi}\right)^2\right)_{\eta=\eta_r}\mathrm{d}\xi\right] + \frac{b}{2}\sum_{r=1}^{n_y}\left[\int_0^1\left(\frac{EI_{y_r}}{b^2}\left(\frac{\partial \psi_\eta}{\partial \eta}\right)^2 + K_{y_r}A_{wy_r}G\left(\frac{\partial w}{b\partial \eta} - \psi_\eta\right)^2 + \frac{GJ_{y_r}}{b^2}\left(\frac{\partial \psi_\xi}{\partial \eta}\right)^2\right)_{\xi=\xi_r}\mathrm{d}\eta\right] \quad (12)$$

$$T_s = \frac{a}{2}\sum_{r=1}^{n_x}\left[\int_0^1\left\{\rho I_{Rx_r}\left(\frac{\partial \psi_\xi}{\partial t}\right)^2 + \rho A_{wx_r}\left(\frac{\partial w}{\partial t}\right)^2\right\}_{\eta=\eta_r}\mathrm{d}\xi\right] + \frac{b}{2}\sum_{r=1}^{n_y}\left[\int_0^1\left\{\rho I_{Ry_r}\left(\frac{\partial \psi_\eta}{\partial t}\right)^2 + \rho A_{wy_r}\left(\frac{\partial w}{\partial t}\right)^2\right\}_{\xi=\xi_r}\mathrm{d}\eta\right] \quad (13)$$

where n_x and n_y represent the number of stiffeners in the x and y direction, respectively. K is the shear coefficient, and A and I_R are the area and the rotary moment of inertia of the stiffener cross-section, respectively. Further, GJ is torsional stiffness while EI is the bending stiffness of the stiffener, considering the plate flange contribution of effective width s as shown in Fig. 2.

If a plate with partial stiffeners (carlings) is considered, Fig. 3, the potential and kinetic energy yield

$$T_s = \frac{a}{2}\sum_{r=1}^{n_x}\left[\int_0^1 \left\{\rho I_{Rx_r}\left(\frac{\partial \psi_\xi}{\partial t}\right)^2 + \rho A_{wx_r}\left(\frac{\partial w}{\partial t}\right)^2\right\}_{\eta=\eta_r} \mathrm{d}\xi\right] + \frac{b}{2}\sum_{r=1}^{n_y}\left[\int_0^1 \left\{\rho I_{Ry_r}\left(\frac{\partial \psi_\eta}{\partial t}\right)^2 + \rho A_{wy_r}\left(\frac{\partial w}{\partial t}\right)^2\right\}_{\xi=\xi_r} \mathrm{d}\eta\right] \tag{14}$$

$$T_s(t) = \frac{a}{2}\sum_{r=1}^{n_x}\left[\int_{a\xi}^{b\xi} \left\{\rho I_{Rx_r}\left(\frac{\partial \psi_\xi}{\partial t}\right)^2 + \rho A_{wx_r}\left(\frac{\partial w}{\partial t}\right)^2\right\}_{\xi=\xi r} d\xi\right] + \frac{b}{2}\sum_{r=1}^{n_y}\left[\int_{a\eta}^{b\eta} \left\{\rho I_{Ry_r}\left(\frac{\partial \psi_\eta}{\partial t}\right)^2 + \rho A_{wy_r}\left(\frac{\partial w}{\partial t}\right)^2\right\}_{\eta=\eta r} d\eta\right] \tag{15}$$

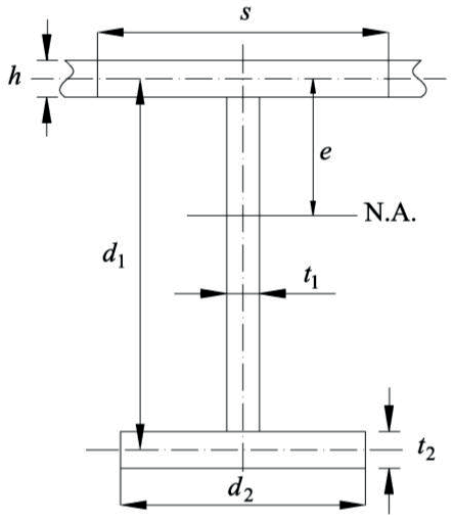

Fig. 2. Cross-section of a stiffener [21]

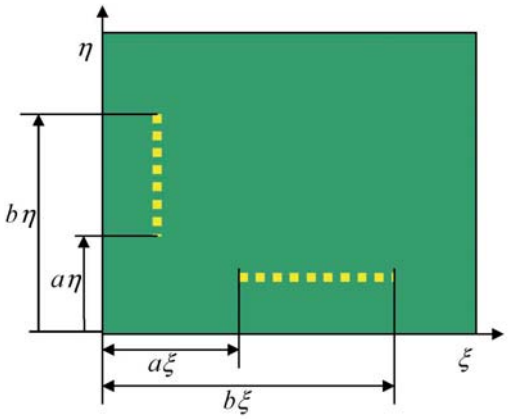

Figure 3 Plate with partial stiffeners

Outline of the assumed mode method

In the assumed mode method, lateral displacement and rotational angles are expressed by superposing the products of the orthogonal polynomials:

$$\begin{aligned} w(\xi,\eta,t) &= \sum_{m=1}^{M}\sum_{n=1}^{N} a_{mn}(t) X_m(\xi) Y_n(\eta), \\ \psi_\xi(\xi,\eta,t) &= \sum_{m=1}^{M}\sum_{n=1}^{N} b_{mn}(t) \Theta_m(\xi) Y_n(\eta), \\ \psi_\eta(\xi,\eta,t) &= \sum_{m=1}^{M}\sum_{n=1}^{N} c_{mn}(t) X_m(\xi) \Phi_n(\eta) \end{aligned} \tag{16}$$

where $X_m(\xi)$, $Y_n(\eta)$, $\Theta_m(\xi)$ and $\Phi_n(\eta)$ are the orthogonal polynomials satisfying the specified elastic edge constraints with respect to ξ and η [8], [16], [21]. Furthermore, $a_{mn}(t)$, $b_{mn}(t)$ and $c_{mn}(t)$ are the influence coefficients of orthogonal polynomials. Also, M and N are the number of orthogonal polynomials used for an approximate solution in the ξ and η directions, respectively. Equations (16) can be alternatively written in matrix form:

$$\{z(\xi,\eta,t)\} = [H(\xi,\eta)]\{q(t)\} \tag{17}$$

where:

$$\{z(\xi,\eta,t)\} = \{w(\xi,\eta,t),\ \psi_\xi(\xi,\eta,t),\ \psi_\eta(\xi,\eta,t)\}^T \tag{18}$$

$$[H(\xi,\eta)] = \begin{bmatrix} X_1Y_1 \ldots X_MY_N & 0 \ldots 0 & 0 \ldots 0 \\ 0 \ldots 0 & \Theta_1Y_1 \ldots \Theta_MY_N & 0 \ldots 0 \\ 0 \ldots 0 & 0 \ldots 0 & X_1\Phi_1 \ldots X_M\Phi_N \end{bmatrix} \tag{19}$$

$$\{q(t)\} = \{a_{11} \ldots a_{MN}\ b_{11} \ldots b_{MN}\ c_{11} \ldots c_{MN}\}^T \tag{20}$$

By substituting equations (1) to (4), depending on the system topology, into Lagrange's equation of motion

$$\frac{\mathrm{d}}{\mathrm{d}t}\left(\frac{\partial T}{\partial \dot{q}_i}\right) - \frac{\partial T}{\partial q_i} + \frac{\partial V}{\partial q_i} = 0 \tag{21}$$

the discrete matrix equation with 3xMxN degrees of freedom is obtained as the following equation:

$$[M]\left\{\frac{\partial^2 q(t)}{\partial t^2}\right\} + [K]\{q(t)\} = 0 \tag{22}$$

where [M] and [K] are the mass matrix and the stiffness matrix, respectively [8], [16], [21]. Their constitution using characteristic orthogonal polynomials is described in detail in [8]. The procedure for the constitution of the stiffness and mass matrices of the attached stiffeners using the same polynomials can also be found in [21].

If we assume harmonic vibrations i.e.

$$\begin{aligned} \{q(t)\} &= \{Q\}e^{j\omega t}, \\ w(\xi,\eta,t) &= W(\xi,\eta)e^{j\omega t}, \\ \psi_\xi(\xi,\eta,t) &= \Psi_\xi(\xi,\eta)e^{j\omega t}, \\ \psi_\eta(\xi,\eta,t) &= \Psi_\eta(\xi,\eta)e^{j\omega t} \end{aligned} \tag{23}$$

equation (22) leads to an eigenvalue problem which gives the natural frequencies and eigenvectors of the system, where j is the imaginary unit and ω represents the angular frequency. The mode shape corresponding to each natural frequency is obtained from the following equation:

$$\left\{W(\xi,\eta),\ \Psi_{\xi}(\xi,\eta),\ \Psi_{\eta}(\xi,\eta),\right\}_{l}^{T} = \left[H(\xi,\eta)\right]\{Q\}_{l} \qquad (24)$$

where l represents the order of the mode. It should be noted here that when using the assumed mode method, the orthogonal polynomials corresponding to the property of the target model should be applied to achieve accurate analysis. For this purpose, the characteristic orthogonal polynomials having the property of Timoshenko beam functions which satisfies the specified edge constraints are used. Their complete derivation is presented in [8], [21].

VAPS software

Based on the above described procedure VAPS software for the vibration analysis of plate systems has been developed. Its current version is applicable for the free vibration analysis of thin and thick rectangular plates and stiffened panels with and without openings and with all possible combinations of boundary conditions. VAPS is executed using Windows OS and has graphical user interface which enables almost instantaneous model preparation, Fig. 4. Also, postprocessing of the results and report preparation are very simple and fast. The software was initially developed for the naval architecture purposes and therefore the software automatically checks the compliance of the dynamic response with the rule-based values prescribed by the relevant classification societies, Fig. 5.

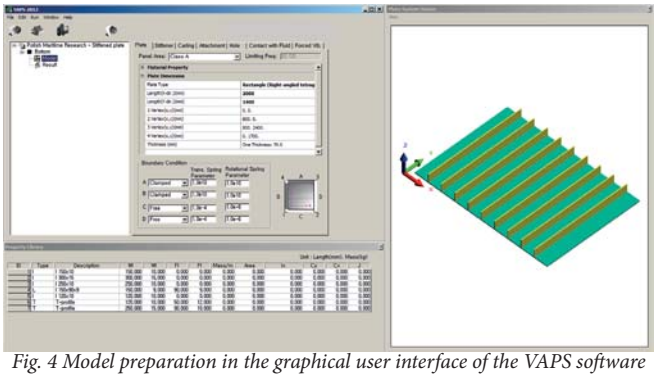

Fig. 4 Model preparation in the graphical user interface of the VAPS software

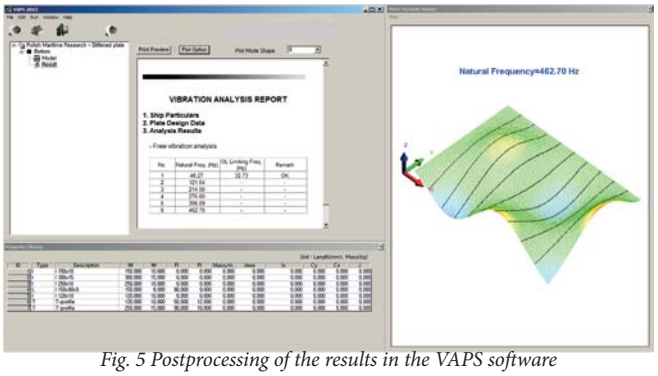

Fig. 5 Postprocessing of the results in the VAPS software

ILLUSTRATIVE NUMERICAL EXAMPLES

The developed procedure is verified with several numerical examples, where different framing (transverse, longitudinal, mixed), plate thicknesses, and holes of different shapes and sizes are included. In the numerical examples, various boundary conditions are also applied. In all calculations, the values of Young's modulus, material density and Poisson's ratio are set to 2.1×10^{11} N/m2, 7850 kg/m^3 and 0.3, respectively. Furthermore, the value of the shear factor k is adjusted to 5/6 and the number of polynomials is set to 13, for both ξ and η directions, respectively. In the proposed procedure, the beam theory is applied in order to take into account the effect of stiffeners. Therefore, in all calculations the stiffeners are modelled as beam elements in the FE analysis, since a comparison of the results in that case is the most realistic. The results obtained by the VAPS software are denoted with PS (Present Solution) in all numerical examples. Also the designated boundary conditions of clamped, simple and free are denoted by C, S and F, respectively.

Thick rectangular plate

The vibration analysis of thick square and rectangular plates using the assumed mode method was already performed by Kim et al. [8], using the in-house MATLAB code. In [8] SSSS, SCSC, CCCC and SSFS boundary conditions were taken into account and very good agreement with FEM results was obtained. Here, the VAPS software is applied to a plate with length equal to 2.0 m and width equal to 1.6 m, and FFSS edge constraints. The obtained results together with FEM solutions obtained with NASTRAN [26] are presented in Table 1, and the mode shapes are shown in Fig. 6.

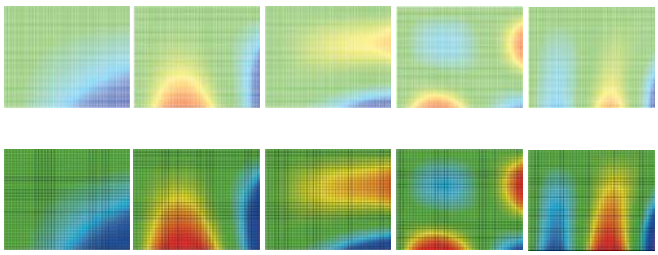

Fig. 6. Mode shapes of a rectangular plate, h/a = 0.1, FFSS

Tab. 1, Natural frequency f (Hz) of rectangular plate, FFSS

Mode no.	*h/a*	PS	FEM	Diff., %
1	0.01	5.23	5.21	0.38
	0.1	50.88	50.72	1.76
2	0.01	24.44	24.37	0.29
	0.1	232.79	230.68	0.91
3	0.01	33.78	33.70	0.24
	0.1	319.87	322.00	-0.66
4	0.01	60.15	59.83	0.53
	0.1	544.94	540.67	0.79
5	0.01	66.94	66.79	0.22
	0.1	609.64	620.15	-1.69

Plate with holes

A plate with length and width equal to 6.0 m and 4.0 m, respectively, and six rectangular holes with dimensions 0.2 x 0.1 m is considered. Results of the free vibration analysis for FCSC boundary conditions and different relative plate thickness h/b are given in Table 2, where very good agreement of the results is obvious. In the case of the first mode which appears as the most relevant for structural design, discrepancies between VAPS and NASTRAN are within 0.5%. Bird's eye views on the first three natural modes of plate flexural vibrations are presented in Fig. 7 and, as expected, very good agreement in this case also is obvious.

Tab. 2. Natural frequency f (Hz) of rectangular plate with six rectangular holes, FCSC

Mode no.	*h/b*	PS	FEM	Diff., %
1	0.01	6.87	6.85	0.29
	0.1	65.99	65.68	0.47
2	0.01	14.81	14.57	1.65
	0.1	139.04	136.76	1.67
3	0.01	18.58	17.83	4.21
	0.1	166.62	166.40	0.13

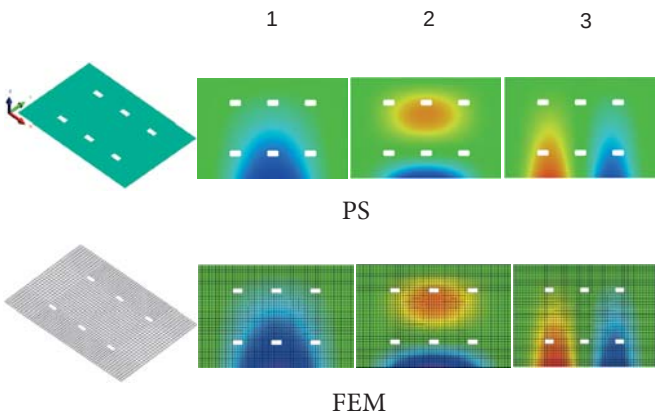

Fig. 7. Models and mode shapes of a rectangular plate with six rectangular holes, h/b = 0.01, FCSC

Stiffened panel

The free vibration analysis of the stiffened panel with mixed framing (cross-stiffened panel) and FFCC boundary conditions was conducted, where the effective widths of stiffeners to evaluate the moment of inertia of the beam cross-section were set to the frame intervals. The panel length and width is 5.0 m and 2.5 m, respectively, while the plate thickness is equal to 0.025 m. The same panel, but with different boundary conditions is analysed in [21]. The stiffeners in longitudinal direction are I profiles with height of 120 mm and width of 10 mm, and their spacing equal to 0.5 m. For the transverse direction, 4 equidistant stiffeners with I profile 150 x 12 mm are applied. The corresponding FE model is comprised of 320 finite elements (200 plates and 120 beams). The mode shapes are in good agreement with FEM results, same as the natural frequencies, Fig. 8.

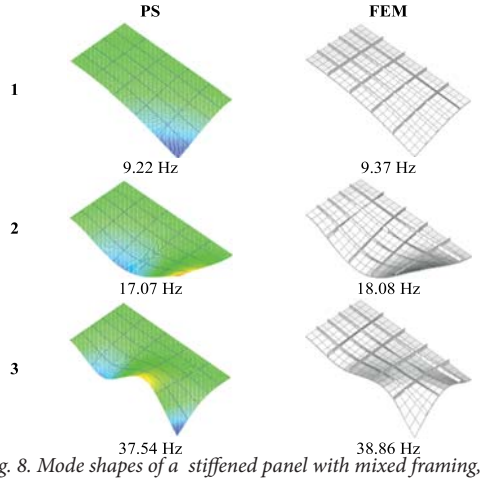

Fig. 8. Mode shapes of a stiffened panel with mixed framing, FFCC

Stiffened panel with holes

The free vibration analysis of a stiffened panel with oval holes and transverse stiffeners is performed using both VAPS and NASTRAN software. The panel length and width are 4.0 m and 3.2 m, respectively, and the dimensions of the holes are 800 x 600 mm. Three equidistant stiffeners are I profiles with height of 250 mm and width of 10 mm, while the thickness of the panel plate is 15 mm. In this case the corresponding FE model consists of 1150 elements (1072 plates and 78 beams). The natural frequencies and mode shapes for the FCSC boundary conditions are shown in Fig. 9, where very good agreement is also achieved.

In the next numerical example, a stiffened panel with length of 14.0 m and width of 10.0 m. The longitudinal framing (1300 x 15) and six circular holes are considered. The thickness of the plate is 50 mm and the hole diameter is equal to 1000 mm. The FE model of the longitudinally stiffened panel consists of 4100 plate and 280 beam finite elements. The CFCC boundary condition is considered. The natural frequencies of the stiffened panel with circular holes and longitudinal stiffeners are presented in Fig. 10 and the agreement of the results is also good, as was the case in the previous numerical examples.

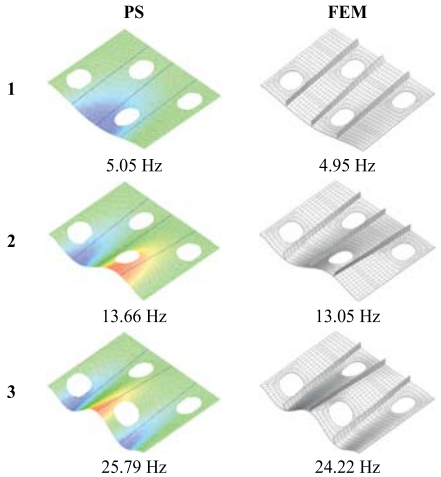

Fig. 9. Mode shapes of a stiffened panel with oval holes and transverse framing, FCSC

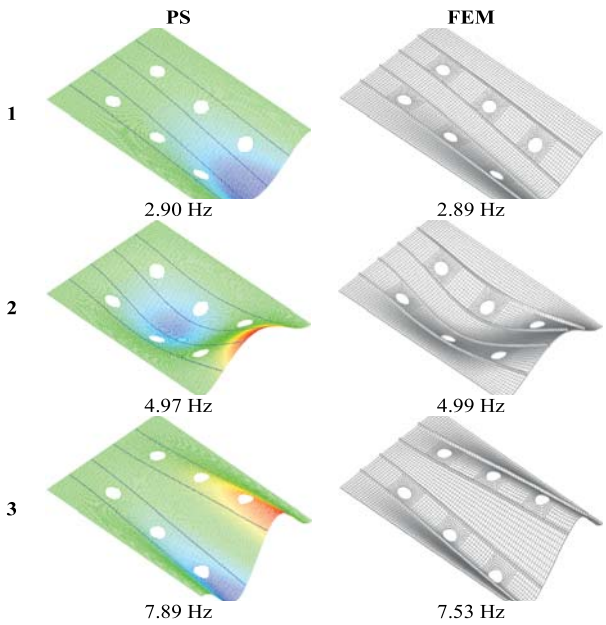

Fig. 10. Mode shapes of a stiffened panel with circular holes and longitudinal framing, CFCC

CONCLUSION

Application of the assumed mode method to free vibration analysis of different plate systems is reviewed. The developed simplified procedure, based on the energy approach, can be applied to thin and thick plates and stiffened panels with and without holes, respectively. Total potential and kinetic energy should be expressed in a convenient manner depending on the system topology. Based on the Lagrange's equation the governing system of matrix equations is derived. Comparisons with FEM results show that the method is very accurate from an engineering point of view. It should be noted that the method can consider all types of boundary conditions and different relative thicknesses of plates, as well as various framings and hole shapes. Short description of the in-house VAPS software is also provided in the paper. The VAPS software is very user-friendly and can be used for fast model preparation, solving of the eigenvalue problem, and postprocessing of the results.

Future investigations should be oriented to the extension of the developed software package VAPS to the vibration analysis of orthotropic plates assuming different materials, and to more complex structural parts of ships and offshore structures, such as, for instance, stiffened panels with additional attachments (lumped inertia and stiffness elements), thick plates and stiffened panels immersed in the water, etc. Also forced response will be considered.

ACKNOWLEDGEMENTS

This work was supported by a National Research Foundation of Korea (NRF) grant funded by the Korean Government (MSIP) through GCRC-SOP (Grant No. 2011-0030013).

BIBLIOGRAPHY

1. [1]Reissner E.: The effect of transverse shear deformation on the bending of elastic plate. Transactions of ASME Journal of Applied Mechanics, 12, (1945), pp. 69-77
2. Mindlin R. D.: Influence of rotary inertia and shear on flexural motions of isotropic elastic plates. Journal of Applied Mechanics, 18, 1(1951), pp. 31-38
3. Liew K. M., Xiang Y., Kitipornchai S.: Research on thick plate vibration: a literature survey. Journal of Sound and Vibration, 180, (1995), pp. 163-176
4. Senjanović I., Vladimir N., Tomić M.: An advanced theory of moderately thick plate vibrations. Journal of Sound and Vibration, 332, (2013), pp. 1868-1880
5. Senjanović I., Tomić M., Vladimir N.: Cho D. S.: Analytical solution for free vibrations of a moderately thick rectangular plate. Mathematical Problems in Engineering, 2013, (2013), Article ID 207460
6. Liew K. M., Xiang Y., Kitipornchai S.: Transverse vibration of thick plates – I. Comprehensive sets of boundary conditions. Computers and Structures, 49, (1993), pp. 1-29
7. Dawe D. J., Roufaeil O. L.: Rayleigh-Ritz vibration analysis of Mindlin plates. Journal of Sound and Vibration, 69, 3(1980), pp. 345-359
8. Kim K.H., Kim B.H., Choi T.M., Cho D.S.: Free vibration analysis of rectangular plate with arbitrary edge constraints using characteristic orthogonal polynomials in assumed mode method. International Journal of Naval Architecture and Ocean Engineering, 4, (2012), pp. 267-280
9. Chung J.H., Chung T.Y., Kim K.C.: Vibration analysis of orthotropic Mindlin plates with edges elastically restrained against rotation. Journal of Sound and Vibration, 163, (1993), pp. 151-163
10. Auricchio F., Taylor R.L.: A triangular thick plate finite element with an exact thin limit. Finite Elements in Analysis and Design, 19, (1995), pp. 57-68
11. Lovadina C.: Analysis of a mixed finite element method for the Reissner-Mindlin plate problems. Computer Methods in Applied Mechanics and Engineering, 163, (1998), pp. 71-85
12. Hughes T.J.R., Tezduyar T.: Finite elements based upon Mindlin plate theory with particular reference to the four-node isoparametric element. Journal of Applied Mechanics, 48, (1981), pp. 587-596

13. Bletzinger K., Bischoff M., Ramm E.: A unified approach for shear-locking free triangular and rectangular shell finite elements. Computers and Structures, 75, (2000), pp. 321-334

14. Nguyen-Xuan H., Liu G. R., Thai-Hong C.: Nguyen-Thoi T. An edge-based smoothed finite element method (ES-FEM) with stabilized discrete shear gap technique for analysis of Reissner-Mindlin plates. Computer Methods in Applied Mechanics and Engineering, 199, (2010), pp. 471-489

15. Senjanović I., Vladimir N., Hadžić N. Modified Mindlin plate theory and shear locking-free finite element formulation. Mechanics Research Communications, 55, (2014), pp. 95-104

16. Cho D.S., Vladimir N., Choi T.M.: Approximate natural vibration analysis of rectangular plates with openings using assumed mode method. International Journal of Naval Architecture and Ocean Engineering, 5, 3(2013), pp. 478-491

17. Paramasivam P.: Free vibration of square plates with openings. Journal of Sound of Vibration, 30, (1973), pp. 173-178

18. Kwak M.K., Han S.: Free vibration analysis of rectangular plate with a hole by means of independent coordinate coupling method. Journal of Sound of Vibration, 306, (2007), pp. 12-30

19. Grossi R.O., del V. Arenas B., Laura P.A.A.: Free vibration of rectangular plates with circular openings. Ocean Engineering, 24, 1(1997), pp. 19-24

20. Monahan L.J., Nemergut P.J., Maddux G.E.: Natural frequencies and mode shapes of plates with interior cut-outs. The Shock and Vibration Bulletin, 41, (1970), pp. 37-49

21. Cho D.S., Vladimir N., Choi T.M.: Natural vibration analysis of stiffened panels with arbitrary edge constraints using the assumed mode method. Proceedings of the IMechE, Part M: Journal of Engineering for the Maritime Environment, (2014), DOI: 10.1177/1475090214521179, published online

22. Samanta A., Mukhopadhyay M.: Free vibration analysis of stiffened shells by the finite element technique. European Journal of Mechanics, A Solids, 23, (2004), pp. 159-179

23. Sivasubramonian B., Kulkarni A. M., Rao G.V.; Krishnan A.: Free vibration of curved panels with cutouts. Journal of Sound and Vibration, 200, (1997), pp. 227-234

24. Sivasubramonian B., Rao G.V., Krishnan A.: Free vibration of longitudinally stiffened curved panels with cutout. Journal of Sound and Vibration, 226, 1(1999), pp. 41-55

25. Srivastava A.K.L.: Vibration of stiffened plates with cutout subjected to partial edge loading. Journal of the Institution of Engineers (India) Series A, 93, 2(2012), pp. 129-135

26. MSC. MD Nastran 2010 Dynamic analysis user's guide. MSC Software, 2010

CONTACT WITH AUTHOR

Dae Seung Cho
Pusan National University
63 beon-gil, Busandaehak-ro
Geumjeong-gu, Busan, 609-735
Korea

daecho@pusan.ac.kr

Nikola Vladimir
University of Zagreb
Faculty of Mechanical Engineering and Naval Architecture
Ivana Lucica 5, 10000 Zagreb,
Croatia

nikola.vladimir@fsb.hr

Tae Muk Choi
Createch Co. Ltd.
Rm. 206, 11 Engineering Bldg.
San 30, Jangjeon 2-dong, Gumjeong-gu,
Busan, 609-735
Korea

taemuk@createch.co.kr